Single-cell analysis implicates T_H17-to-T_H2 cell plasticity in the pathogenesis of palmoplantar pustulosis

Daniel McCluskey, MSc,[a] Natashia Benzian-Olsson, MSc,[a] Satveer K. Mahil, PhD,[b] Niina Karoliina Hassi, MSc,[a] Christian T. Wohnhaas, PhD,[c] for the APRICOT and PLUM study team,* A. David Burden, MD,[d] Christopher E. M. Griffiths, MD,[e] John R. Ingram, MD,[f] Nick J. Levell, MD,[g] Richard Parslew, MD,[h] Andrew E. Pink, MD,[b] Nick J. Reynolds, MD,[i] Richard B. Warren, PhD,[e] Sudha Visvanathan, PhD,[j] Patrick Baum, PhD,[c] Jonathan N. Barker, MD,[b] Catherine H. Smith, MD,[b] and Francesca Capon, PhD[a] *London, Manchester, Norwich, Liverpool, Newcastle upon Tyne, Glasgow, and Cardiff, United Kingdom; Biberach, Germany; and Ridgefield, Conn*

GRAPHICAL ABSTRACT

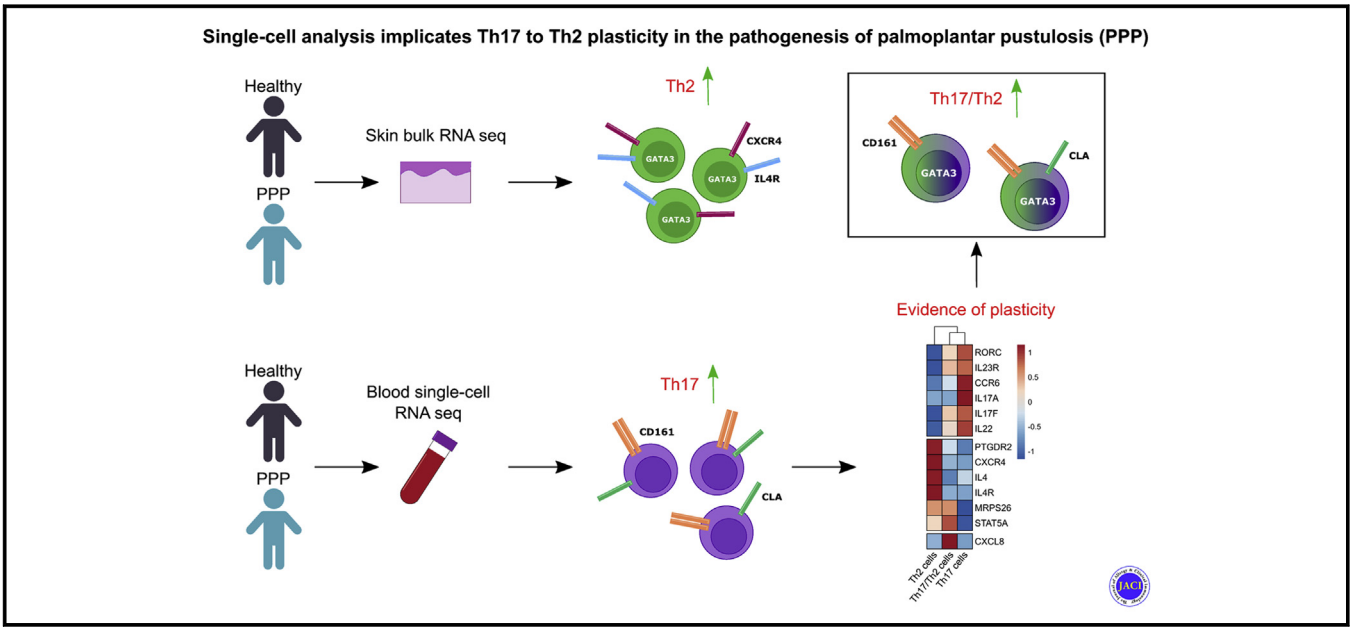

Background: Palmoplantar pustulosis (PPP) is a severe inflammatory skin disorder characterized by eruptions of painful, neutrophil-filled pustules on the palms and soles.

Although PPP has a profound effect on quality of life, it remains poorly understood and notoriously difficult to treat.

From [a]the Department of Medical and Molecular Genetics and [b]the St John's Institute of Dermatology, Faculty of Life Sciences and Medicine, King's College London, London; [c]Boehringer Ingelheim Pharma GmbH & Co KG, Biberach; [d]the Institute of Infection Immunity and Inflammation, University of Glasgow, Glasgow; [e]the Dermatology Centre, Salford Royal National Health Service (NHS) Foundation Trust, National Institute for Health Research (NIHR) Manchester Biomedical Research Centre, University of Manchester, Manchester; [f]the Department of Dermatology, Division of Infection & Immunity, Cardiff University, Cardiff; [g]Norwich Medical School, University of East Anglia, Norwich; [h]Department of Dermatology, Royal Liverpool Hospitals, Liverpool; [i]Translational and Clinical Research Institute, Newcastle University and Department of Dermatology and NIHR Newcastle Biomedical Research Centre, Newcastle Hospitals NHS Foundation Trust, Newcastle upon Tyne; and [j]Boehringer Ingelheim Pharmaceuticals, Ridgefield.

*Further members of the APRICOT and PLUM study team are listed in the acknowledgments.

The bulk and single-cell RNA sequencing data we report here have been uploaded to the publicly accessible Gene Expression Omnibus repository (www.ncbi.nlm.nih.gov/geo; series accession no. GSE185858).

Support was received from the Department of Health via the NIHR BioResource Clinical Research Facility and comprehensive Biomedical Research Centre awards to Guy's and St Thomas' NHS Foundation Trust in partnership with King's College London and King's College Hospital NHS Foundation Trust (guysbrc-2012-1). Support was also received from the Newcastle NIHR Biomedical Research Centre. The APRICOT trial was funded by the Efficacy and Mechanism Evaluation (EME) Programme, a UK Medical Research Council (M.R.C.) and NIHR partnership (grant EME 13/50/17 to C.H.S., F.C., J.N.B., A.D.B., R.B.W., N.J.R., and C.E.M.G.). This work was also supported by the European Academy of Dermatology and Venereology (grant PPRC-2018-25 to F.C. and J.N.B.) and the Psoriasis Association (grant BSTOP50/5 to C.H.S.). D.Mc. is supported by the Medical Research Council (MRC; grant MR/R015643/1) and King's College London as member of the MRC Doctoral Training Partnership in Biomedical Sciences. N.B.O. was funded by a NIHR predoctoral fellowship (grant NIHR300473). S.K.M. is funded by an MRC Clinical Academic Research Partnership award (MR/T02383X/1). C.E.M.G. is funded in part by the NIHR Manchester Biomedical Research Centre and is an NIHR emeritus senior investigator. N.J.R. is an NIHR senior investigator. He acknowledges support from the Newcastle MRC/EPSRC Molecular Pathology Node and the Newcastle NIHR Medtech and *In Vitro* Diagnostic Co-operative. R.B.W. is

Objective: We sought to investigate the immune pathways that underlie the pathogenesis of PPP.
Methods: We applied bulk and single-cell RNA sequencing (RNA-Seq) methods to the analysis of skin biopsy samples and peripheral blood mononuclear cells. We validated our results by flow cytometry and immune fluorescence microscopy
Results: Bulk RNA-Seq of patient skin detected an unexpected signature of T-cell activation, with a significant overexpression of several T_H2 genes typically upregulated in atopic dermatitis. To further explore these findings, we carried out single-cell RNA-Seq in peripheral blood mononuclear cells of healthy and affected individuals. Memory $CD4^+$ T cells of PPP patients were skewed toward a T_H17 phenotype, a phenomenon that was particularly significant among cutaneous lymphocyte-associated antigen–positive skin-homing cells. We also identified a subset of memory $CD4^+$ T cells that expressed both T_H17 (*KLRB1*/CD161) and T_H2 (*GATA3*) markers, with pseudotime analysis suggesting that the population was the result of T_H17 to T_H2 plasticity. Interestingly, the $GATA3^+$/$CD161^+$ cells were overrepresented among the peripheral blood mononuclear cells of affected individuals, both in the single-cell RNA-Seq data set and in independent flow cytometry experiments. Dual-positive cells were also detected in patient skin by immune fluorescence microscopy.
Conclusions: PPP is associated with complex T-cell activation patterns and may explain why biologic drugs that target individual T helper cell populations have shown limited therapeutic efficacy. (J Allergy Clin Immunol 2022;150:882-93.)

Key words: *Single-cell RNA sequencing, scRNA-Seq, T-cell plasticity, palmoplantar pustulosis, PPP*

Abbreviations used
CLA: Cutaneous lymphocyte-associated antigen
FDR: False discovery rate
HC: Healthy control
NL: Nonlesional
PBMC: Peripheral blood mononuclear cell
PPP: Palmoplantar pustulosis
RNA-Seq: RNA sequencing
scRNA-Seq: Single-cell RNA-Seq
UMAP: Uniform manifold approximation and projection

Palmoplantar pustulosis (PPP) is a chronic and debilitating skin disorder that manifests as the eruption of neutrophil-filled pustules on the palms and soles. These painful lesions typically occur on a background of inflamed skin, causing functional and occupational disability.[1]

PPP has a profound impact on quality of life, but its causes remain poorly understood. The disease preferentially affects adult female subjects and is associated with cigarette smoking.[2] However, the mechanisms mediating the effects of sex and tobacco exposure are unclear.[3] Although it has been suggested that PPP shares common genetic determinants with other pustular diseases, *IL36RN* mutations (which are frequently observed in generalized pustular psoriasis) have only been reported in a small number of cases.[2,4]

As a result of this limited understanding of disease pathogenesis, evidence-based guidelines for the management of PPP are lacking.[5] The response to conventional systemic therapeutics (oral retinoids, methotrexate, and cyclosporine) is variable, and their prolonged use can have toxic effects.[5] Clinical trials of IL-1 (anakinra) and IL-36 (spesolimab) blockers have been carried out on the assumption that PPP has an autoinflammatory pathogenesis, but the studies undertaken so far could not provide evidence of broad clinical efficacy.[6,7] IL-17 (secukinumab) and IL-23 (guselkumab) inhibitors have also been assessed. Although these biologics reduced disease severity, skin clearance was observed in <30% of patients.[8,9]

We therefore sought to identify disease drivers and potential therapeutic targets for PPP via transcription profiling of patient cells. We uncovered a complex immunologic landscape, where T_H2 cell activation dominates in skin while circulating T cells are skewed toward a T_H17 phenotype. We also observed evidence of increased T_H17-to-T_H2 plasticity in the circulating and skin-homing T lymphocytes of affected individuals. These findings point to the activation of diverse T helper cell populations in PPP and warrant the investigation of small-molecule therapeutics that can inhibit multiple signaling pathways.

METHODS

Study participants

This work was carried out in accordance with the principles of the declaration of Helsinki and after receipt of written informed consent from all participants. PPP was diagnosed on the bases of the results of clinical examination and the consensus criteria of the European Rare and Severe Psoriasis Expert Network, or ERASPEN.[10] Affected individuals were ascertained through the APRICOT clinical trial (approved by the London Dulwich research ethics committee; reference 16/LO/0436) or its sister research study, PLUM (approved by the London Bridge research ethics committee; reference 16/LO/2190). Age- and sex-matched healthy volunteers were also recruited onto the PLUM study. Clinical and demographic features of study participants are summarized in Table E1 in this article's Online Repository at www.jacionline.org.

supported by the Manchester NIHR Biomedical Research Centre. The views expressed in this publication are those of the authors and not necessarily those of the MRC, NHS, NIHR, or the Department of Health.

Disclosure of potential conflict of interest: F. Capon and J. N. Barker have received funding from Boehringer-Ingelheim. C. T. Wohnhaas, P. Baum and S. Visvanathan are Boehringer-Ingelheim employees. J. R. Ingram is editor in chief of the *British Journal of Dermatology* and receives an author honorarium from UpToDate. He is a consultant for UCB Pharma, Novartis, Boehringer Ingelheim, and ChemoCentryx and participated in advisory boards for Kymera Therapeutics and Viela Bio, all in the field of hidradenitis suppurativa. He is a co-copyright holder of the HiSQOL and Patient Global Assessment instruments for hidradenitis suppurativa. R. B. Warren has received research grant and/or consultancy fees from AbbVie, Almirall, Amgen, Arena, Astellas, Avillion, Biogen, Boehringer Ingelheim, Bristol Myers Squibb, Celgene, DiCE, GSK, Janssen, Lilly, Leo, Medac, Novartis, Pfizer, Sanofi, Sun Pharma, UCB, and UNION. The rest of the authors declare that they have no relevant conflicts of interest.

Received for publication October 20, 2021; revised March 4, 2022; accepted for publication April 20, 2022.
Available online May 12, 2022.

Corresponding author: Francesca Capon, PhD, 9th Floor Tower Wing, Guy's Hospital, London SE1 9RT, United Kingdom. E-mail: francesca.capon@kcl.ac.uk.

The CrossMark symbol notifies online readers when updates have been made to the article such as errata or minor corrections
0091-6749

https://doi.org/10.1016/j.jaci.2022.04.027

Sampling and RNA sequencing of skin biopsy samples

Two-millimeter acral skin biopsy samples were obtained from healthy controls (HCs) or APRICOT trial participants. Patients were recruited at their baseline visit after a recommended washout period and before treatment initiation.[6] Lesional biopsy samples were taken from inflamed skin (avoiding pustules), while nonlesional (NL) samples were taken via biopsy from adjacent uninvolved skin. Total RNA was extracted using a miRVana isolation kit (Thermo Fisher Scientific, Waltham, Mass). After poly-A selection and library preparation, samples were run on an Illumina HiSeq instrument (Illumina, San Diego, Calif) to generate 150 bp paired-end reads.

Single-cell RNA sequencing

Peripheral blood mononuclear cells (PBMCs) were resuspended in fetal calf serum (Invitrogen; Thermo Fisher Scientific)/10% dimethyl sulfoxide and stored in liquid nitrogen for up to 4 weeks. On the day of the experiment, cells were thawed, counted, and loaded on a Chromium Single Cell 3′ Chip (10× Genomics, Pleasanton, Calif), as described elsewhere.[11] Libraries were prepared using the Single Cell 3′ Reagent Kits v3 (10× Genomics) and sequenced on a HiSeq4000 instrument (Illumina).

Data analysis by single-cell RNA sequencing

Sequence reads were processed, aligned to the GRCh38 reference genome, and annotated to Ensembl (release 86) genes by Cell Ranger v3.0.2 software (10× Genomics). The healthy donor data sets published by Zheng et al[12] (n = 3) and Schafflick et al[13] (n = 5) were retrieved from the 10× Genomics portal (support.10xgenomics.com/single-cell-gene-expression/datasets) and the Gene Expression Omnibus repository (www.ncbi.nlm.nih.gov/geo; identifier GSE138266), respectively. The 3 data sets were then merged using Harmony[14] to correct for batch effects. The resulting gene expression matrix was processed with Seurat v3.0.[15] Quality control filters were first applied to remove cells with low (<300) or excessive (>5000) numbers of detected genes. Cells where the percentage of mitochondrial gene reads exceeded 20% were also excluded. After log normalization and data scaling, variation due to the following sources was regressed out: sequencing batch, data origin (Zheng et al, Schafflick et al, and generated in house), smoking status, treatment with biologic agents, and unique molecular identifier.

After principal component analysis and construction of a K-nearest neighbor graph, unsupervised clustering was undertaken with a resolution of 0.4. The resulting cell clusters were visualized by uniform manifold approximation and projection (UMAP). Cluster markers were computed with the FindAllMarkers Seurat function, and cell identities were annotated on the basis of the expression of canonical marker genes. SingleR[16] was used to validate cell identities and to annotate the phenotypes of memory $CD4^+$ T cells as T_H1, T_H2, or T_H17. The full resource published by Monaco et al[17] was used as a reference data set.

For pseudotime analysis, the 3 $CD4^+$ T-cell clusters (naive $CD4^+$, memory $CD4^+$ type 1 [T1], and memory $CD4^+$ type 2 [T2]) were manually retrieved and processed with Slingshot v1.7.0.[18] After UMAP dimensionality reduction with the 'uwot' package, a minimum spanning tree was fitted to the clusters. The resulting trajectory was smoothed by iteratively fitting principal curves.

Statistical analysis

Cell abundance and gene expression levels were compared in cases versus controls by the Mann-Whitney test. The significance of overlaps observed in Venn diagrams was computed by the Fisher exact test. All tests were implemented in R v4.02 (www.r-project.org). $P < .05$ was considered statistically significant.

RESULTS

A prominent T_H2 signature in NL-PPP skin

To explore the immune pathways that are disrupted in PPP, we first carried out bulk RNA sequencing (RNA-Seq) in 3 paired, lesional and NL skin biopsy samples, obtained from the palmar or plantar (acral) skin of affected individuals (Table E1). We identified a total of 1050 differentially expressed genes (log_2 fold change [FC] > |0.5|; false discovery rate [FDR] < 0.05) (see Fig E1, *A,* and Table E2, *A,* in the Online Repository at www.jacionline.org). In keeping with the neutrophilic nature of PPP lesions, these showed a significant enrichment for innate pathways (eg, "granulocyte adhesion and diapedesis" and "IL-8 signaling"; FDR < 10^{-3} for both) (Fig E1, *A*).

We obtained similar results when we compared the 3 lesional samples with healthy acral skin donated by 7 volunteers matched for age, sex, and smoking status (Table E1). In fact, we identified 1323 differentially expressed genes showing a very marked enrichment for innate pathways (eg, "granulocyte adhesion and diapedesis", FDR < 10^{-8}). At the same time, we also uncovered an unexpected overrepresentation of T-cell–related genes (eg, "T-cell receptor signaling", FDR < 10^{-6}) (Fig E1, *B*).

To further explore these findings while avoiding the confounding effects of end-stage inflammation (ie, the secondary upregulation of genes that do not contribute to disease pathogenesis), we next compared NL-PPP biopsy samples (n = 8) with healthy skin (n = 7). We observed 531 differentially expressed genes (Fig 1, *A,* Fig E1, *C,* and Table E2, *B*). In keeping with the results of genetic studies and clinical trials,[2,6] we found limited evidence for a sustained upregulation of IL-36 signaling. While *IL36A* (encoding IL-36α) was overexpressed in NL compared to control skin, the mRNA levels of *IL36B, IL36G,* and *IL1RL2* (encoding, respectively, IL-36β, IL-36γ, and IL-36R) were comparable in the 2 groups.

A closer inspection of the 531 genes that were differentially expressed in NL-PPP skin revealed a pervasive enrichment of T-cell activation pathways (eg, "CD28 signaling in T helper cells" and "Inducible T Cell Costimulator [ICOS]-ICOS Ligand [ICOSL] signaling in T helper cells"; FDR < 10^{-8} for both), with significant evidence for an involvement of T_H2 (FDR = 1.2×10^{-8}), and to a lesser extent T_H1 (FDR = 5.6×10^{-7}), responses (Fig 1, *B,* and see Table E3, *A,* in the Online Repository at www.jacionline.org). Conversely, the enrichment of T_H17-related genes was limited (FDR = 0.001) (Table E3, *A*). In keeping with these observations, an upstream regulator analysis demonstrated a significant overrepresentation of genes induced by IFN-γ, IL-4 (FDR < 10^{-15} for both), and IL-13 (FDR < 10^{-10}) (Fig 1, *C*). This was accompanied by a modest enrichment of IL-17–dependent loci (FDR < 10^{-3}) (Table E3, *B*).

To further explore the significance of these findings, we reanalyzed publicly available skin RNA-Seq data, including data from patients with T_H2- (atopic dermatitis, n = 27) and T_H17- (plaque psoriasis, n = 28) mediated conditions, as well as healthy volunteers (n = 38).[19] We identified 510 genes that were differentially expressed in NL atopic dermatitis skin compared to site-matched control biopsy samples (log_2 FC >|0.5|; FDR < 0.05). When we compared these genes with the 531 that were differentially expressed in NL-PPP skin, we observed a very significant overlap between the 2 data sets (111 shared genes; odds ratio over genomic background, 18.8). While this observation further confirmed the upregulation of T_H2 pathways in PPP skin, the evidence for T_H17 activation was less significant. In fact, there was a limited overlap between the NL-PPP data set and the 630 genes that were differentially expressed in NL psoriasis skin compared to HC (53 shared genes; odds ratio, 5.4) (Fig 1, *D*).

To further validate these findings, we used real-time PCR to analyze uninvolved acral skin obtained from 8 patients with PPP

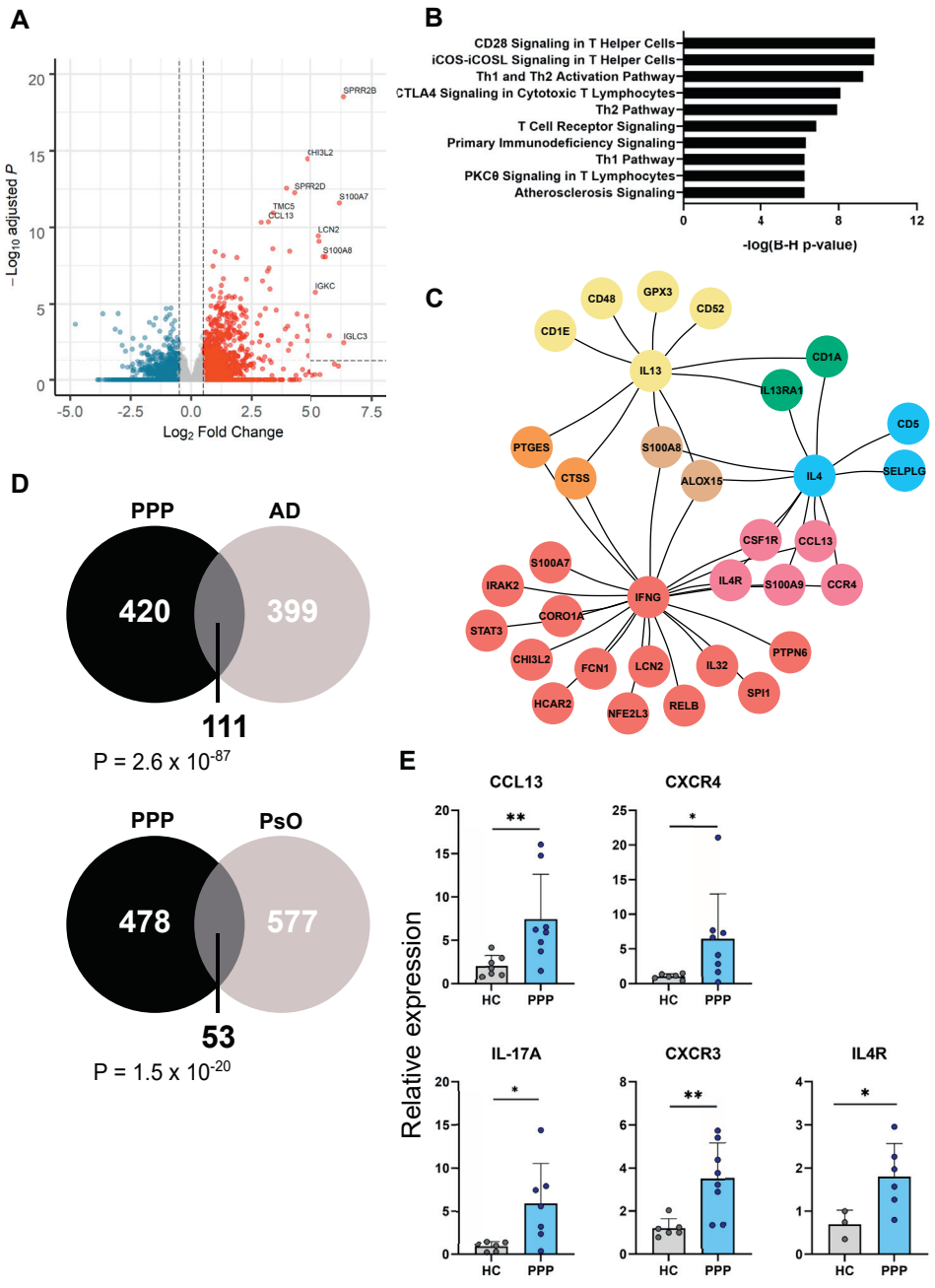

FIG 1. Transcription profiling of NL-PPP skin reveals a prominent T_H2 gene signature. **A,** Volcano plot displaying genes that are differentially expressed in NL versus control skin. *Dotted horizontal lines* and *dotted vertical lines* represent, respectively, significance (FDR < 0.05) and fold change (log_2 FC > |0.5|) thresholds. **B,** The 10 most significantly enriched pathways detected among genes that are differentially expressed in NL-PPP skin. **C,** Hub-and-spoke representation of key upstream regulators (IFN-γ, IL-4, and IL-13) and their over-expressed target genes. **D,** Overlap between the genes differentially expressed in NL-PPP, atopic dermatitis (AD), and psoriasis (Pso) skin. Statistical significance was calculated by Fisher exact test. **E,** Relative mRNA expression of T_H1, T_H2, and T_H17 genes in NL-PPP skin. Data are presented as means ± SDs. Because not all biopsy samples yielded the same amount of mRNA, some samples could not be analyzed for all target genes. *P < .05 (Mann-Whitney test).

and 7 HCs (including 5 patients and 3 HCs who had not been included in the RNA-Seq experiment). This confirmed that key T_H2 genes such as *IL4R, CCL13*/MCP-4 (which activates the CCR3 receptor expressed by T_H2 cells[20]), and *CXCR4* (which is expressed on the surface of T_H2 cells and eosinophils[21]) were upregulated in NL-PPP skin. A moderate increase of T_H1 (*CXCR3*) and T_H17 (*IL17A*) markers was also observed (Fig 1, *E*).

Taken together, these observations identified a marked signature of T_H2 activation in NL-PPP skin, with evidence for a more modest involvement of T_H17 pathways.

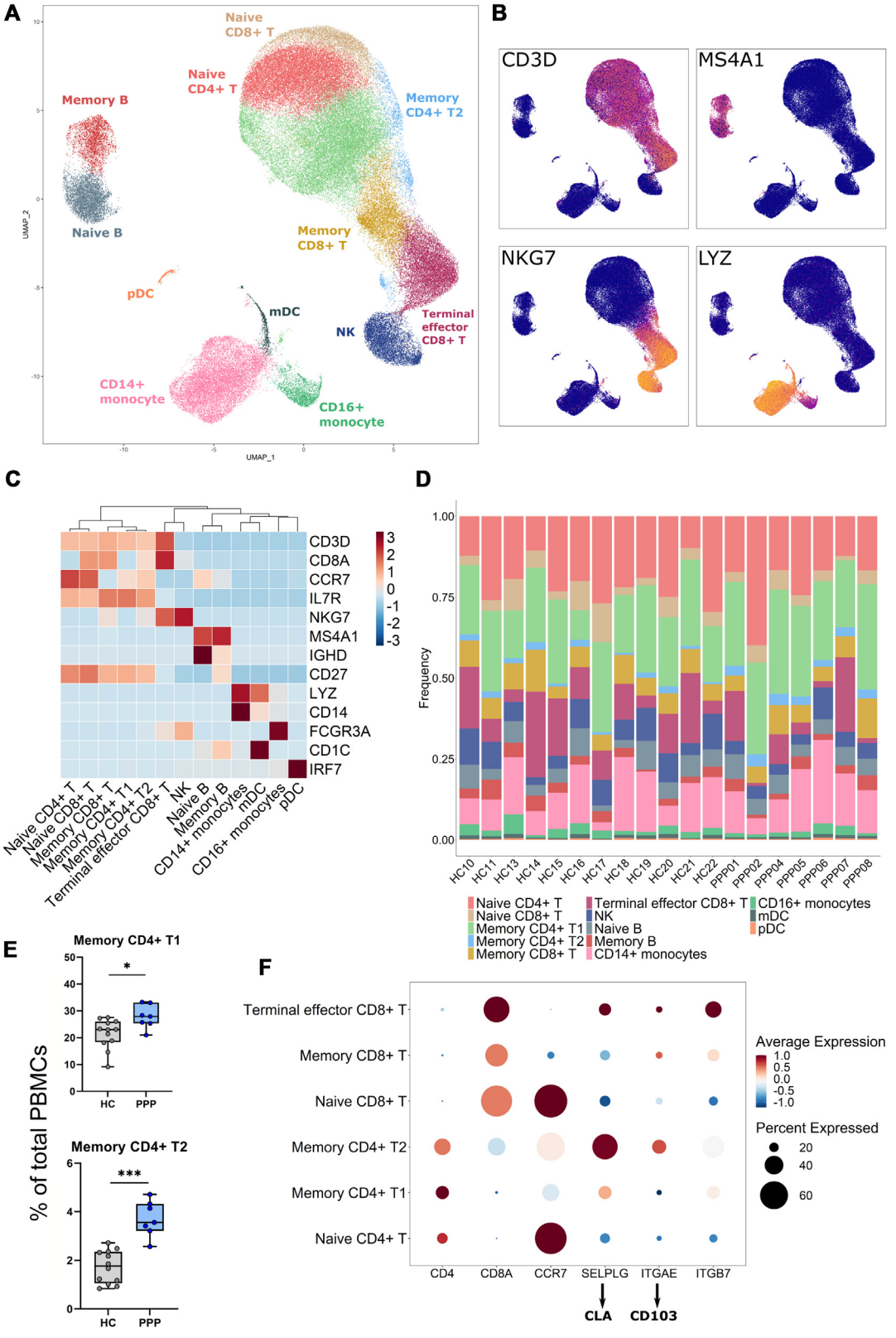

FIG 2. scRNA-Seq of PBMCs reveals an increased abundance of memory CD4$^+$ T cells in PPP patients. **A,** UMAP plot showing that the examined cells (n = 93,262) form 13 separate clusters. *NK,* Natural killer cells. **B,** UMAP plot illustrating the expression of key marker genes in the same 93,262 cells. **C,** Heat map displaying the expression of marker genes across the 13 cell populations. **D,** Stacked bar plot showing the abundance of the 13 cell populations within the PBMCs of each donor. **E,** Increased abundance of memory CD4$^+$ T cell clusters in PPP cases (n = 7) compared to HCs (n = 12). *Box plots* show medians and interquartile ranges; *whiskers* illustrate minimum and maximum values. $^{**}P < .01$, $^{***}P < .001$ (Mann-Whitney test). **F,** Plot showing the expression of key T-cell markers in 6 CD3$^+$ clusters.

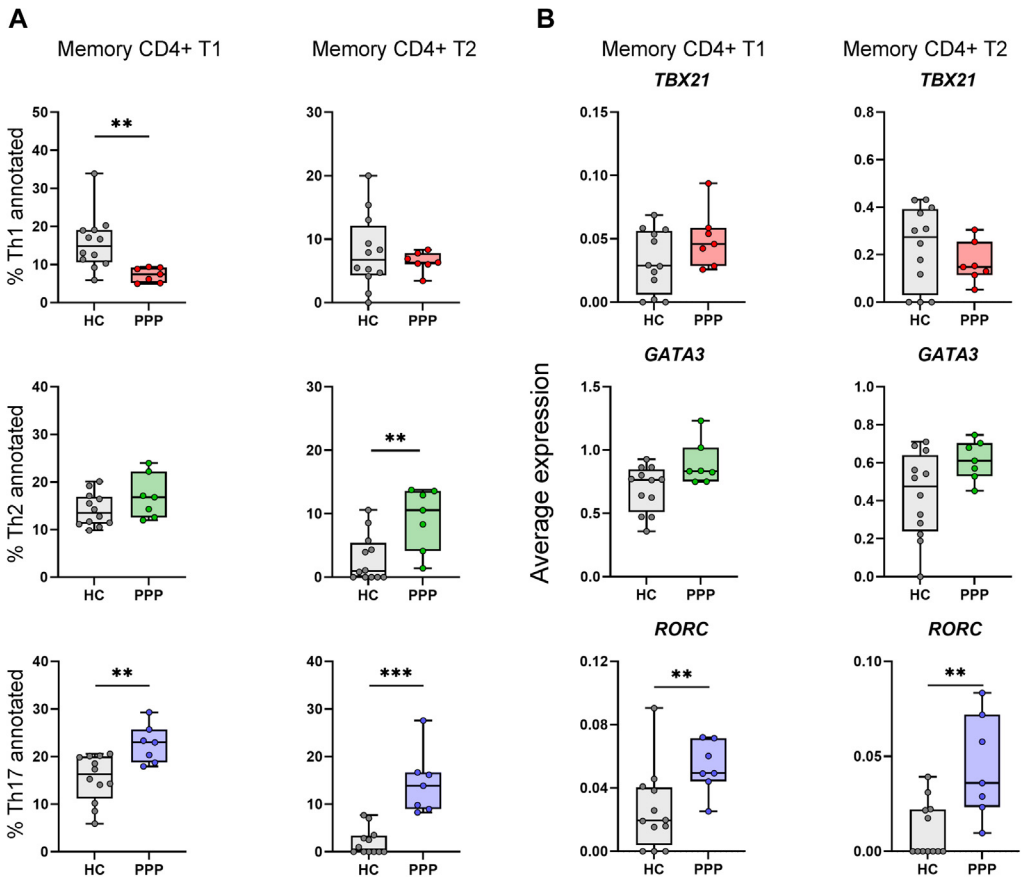

FIG 3. The memory CD4$^+$ T cells of PPP patients are skewed toward a T_H17 phenotype. **A,** Percentage of memory CD4$^+$ T cells annotated as T_H1, T_H2, or T_H17 by SingleR. **B,** Expression (normalized unique molecular identifier counts) of master transcription factors driving T_H1 (*TBX21*), T_H2 (*GATA3*), and T_H17 (*RORC*) differentiation. *Box plots* show medians and interquartile ranges. **P* < .05, ***P* < .01, ****P* < .001 (Mann-Whitney test).

Increased abundance of 2 circulating T-cell subsets in PPP

We next investigated whether systemic immune responses were also deregulated in PPP. We therefore carried out single-cell RNA-Seq (scRNA-Seq) in PBMCs obtained from 7 PPP cases and 4 age- and sex-matched healthy volunteers (Table E1). After capture on a 10× Genomics platform, 3′ end sequencing, and quality control, we observed 58,412 viable cells (see Table E4 in the Online Repository at www.jacionline.org). To maximize statistical power, we expanded this data set by including 8 publicly available control samples, which had been processed on the same platform used in our experiment, yielding comparable cell numbers[12,13] (see Fig E2, *A,* in the Online Repository). To integrate these external HCs in our resource, we undertook batch correction with the Harmony algorithm,[14] obtaining a total of 93,262 cells (Fig 2, *A,* and Fig E2, *B*).

When we analyzed the merged data set with Seurat,[15] we identified 13 cell clusters, which we visualized by uniform manifold approximation and projection (UMAP) (Fig 2, *A,* and Fig E2, *C*). The annotation of cell identities (implemented by manual inspection of canonical marker genes [see Table E5 in the Online Repository at www.jacionline.org] and validated with SingleR[16]) revealed that the clusters corresponded to natural killer cells, monocytes (CD14$^+$ and CD16$^+$ subsets), myeloid and plasmacytoid dendritic cells, B cells (memory and naive subsets), and T cells (2 naive, 1 effector, and 3 memory subsets) (Fig 2, *A-C,* and see Fig E3, *A,* in the Online Repository). Although unconventional T lymphocytes (mucosal-associated invariant T cells and γδ T cells) were also detected, they did not form separate clusters (Fig E3, *B* and *C*).

A comparison of cases and controls showed that innate cells (monocytes, natural killer cells, and dendritic cells) were found at similar frequencies in the 2 groups. Conversely, 2 of the T-cell subsets were more abundant among affected individuals. These corresponded to clusters that we had initially labeled as memory CD4$^+$ T1 (accounting for 27.9% cells in cases vs 23.1% in controls; $P = .02$) and memory CD4$^+$ T2 (3.6% cells in cases vs 1.8% in controls; $P < 10^{-4}$) cells (Fig 2, *D* and *E*). Control cell frequencies were comparable between the samples recruited in house and those retrieved from public databases, showing that the analysis was not skewed by the inclusion of external data sets (Fig E2, *D*).

To further investigate the identity of the 2 CD4$^+$ memory populations, we assessed whether they expressed cutaneous lymphocyte-associated antigen (CLA), a well-known skin-homing marker. We found that cells expressing *SELPLG* (the gene encoding CLA) were a minority among memory CD4$^+$ T1 lymphocytes, but they were very frequent in the CD4$^+$ T2 subset

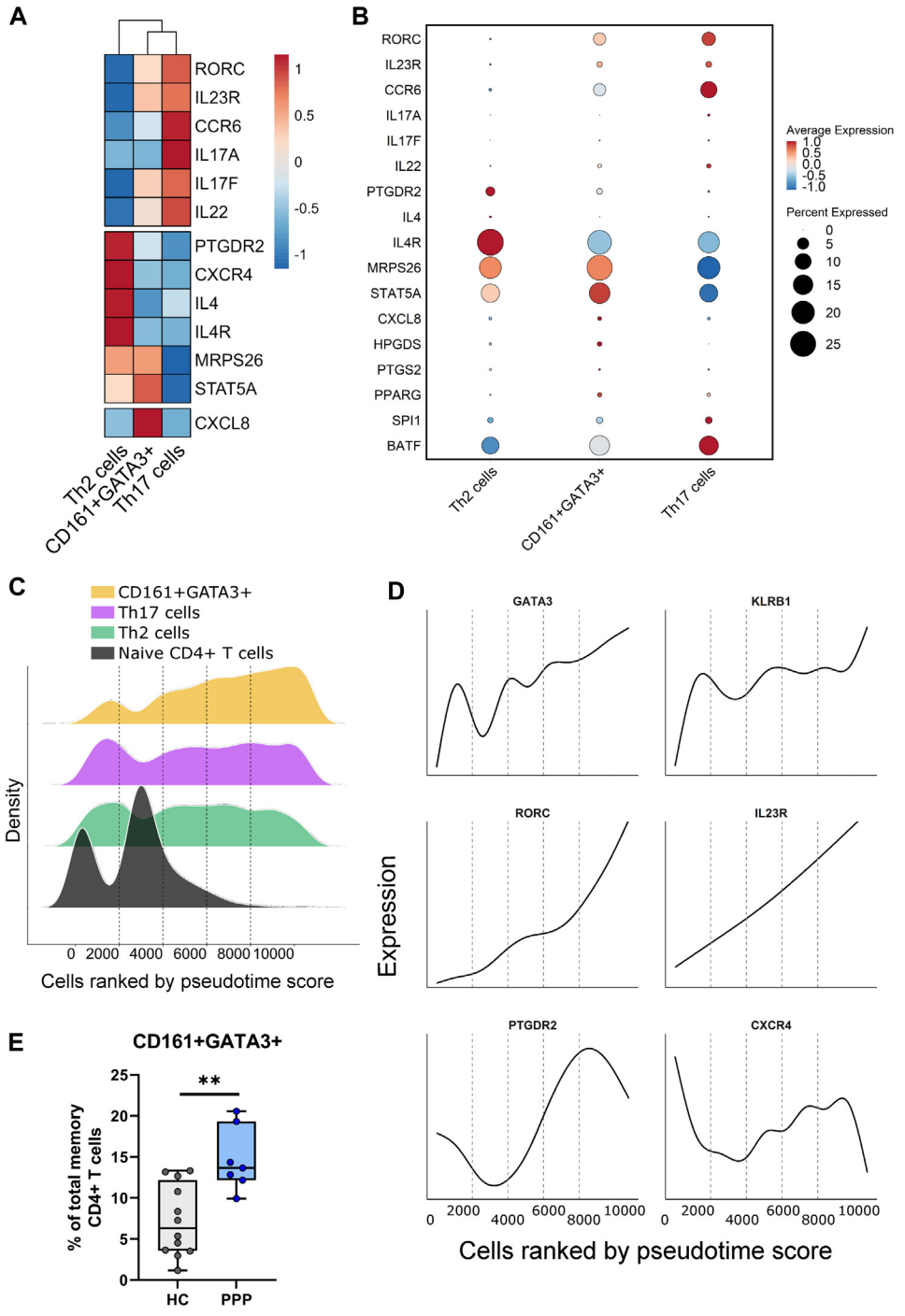

FIG 4. Characterization of GATA3^{+}/CD161^{+} memory CD4^{+} T cells. **A,** Heat map illustrating the expression levels of key marker genes in T_H2, T_H17, and dual-positive cells, selected on the basis of simultaneous GATA3 and CD161 expression. **B,** Bubble plot showing minimal expression of *HPGDS, PTGS2,* and *PPARG* in dual-positive cells. **C,** Histogram illustrating the frequency distribution of T_H2, T_H17, and dual-positive cells during pseudotime analysis. Naive CD4^{+} T cells were included in the analysis as a reference undifferentiated population. **D,** Plots showing the expression of individual marker genes during pseudotime. **E,** Elevated frequency of dual-positive cells in PPP cases compared to HCs. *Box plots* show median and interquartile ranges. $^{**}P < .01$ (Mann-Whitney test).

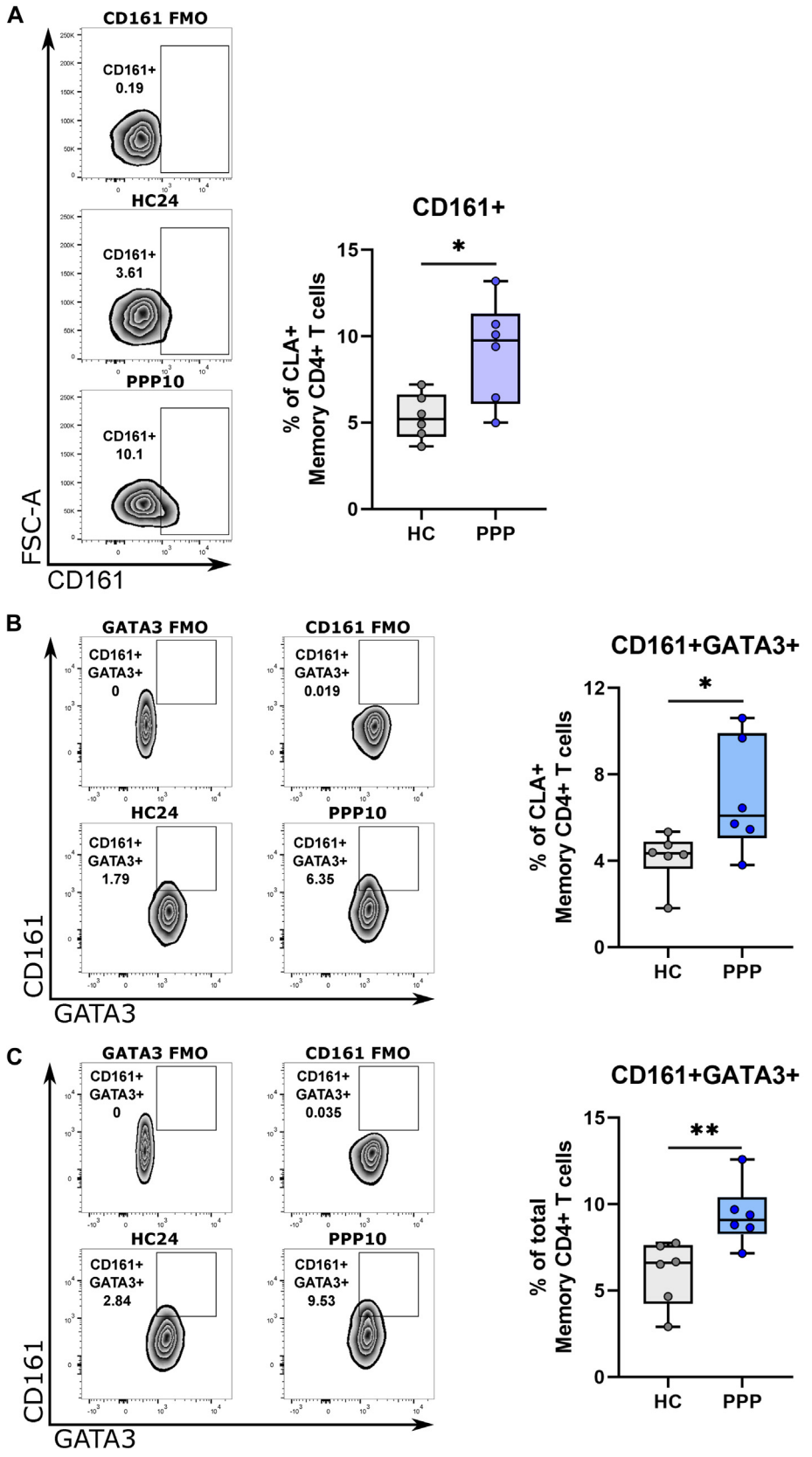

FIG 5. Flow cytometry experiments confirm the elevated frequency of GATA3$^+$/CD161$^+$ memory CD4$^+$ T cells among affected individuals. Comparison of PPP cases (n = 6) and HCs (n = 6) shows (**A**) increased abundance of T_H17 (CD161$^+$) cells among the skin-homing (CLA$^+$) memory CD4$^+$ T cells of affected individuals, (**B**) increased abundance of CD161$^+$GATA3$^+$ cells among skin-homing cells, and (**C**) total memory CD4$^+$ T cells of affected individuals. Memory CD4$^+$ T cells were gated as a CD3$^+$/CD4$^+$/CD45RA− lymphocyte population. Skin-homing cells were identified as a CLA$^+$ subset. Representative contour plots are shown on the left, with fluorescence minus 1 (FMO) negative controls for each antibody. *Box plots* at right show medians and interquartile ranges. *$P < .05$, **$P < .01$ (Mann-Whitney test).

(28.0% vs 51.2% $P < .0001$). Of note, *ITGB7* (encoding the gut-homing receptor integrin β7) was virtually undetectable in the latter population, confirming the specificity of the skin-homing phenotype.

Interestingly, $CD4^+$ T2 cells also expressed *ITGAE,* which encodes the CD103 antigen (Fig 2, *F*). This identifies tissue-resident memory T cells (T_{RM} cells) that have reentered the circulation and are migrating to secondary skin sites.[22] Thus, the memory $CD4^+$ T1 and $CD4^+$ T2 clusters correspond to circulating and skin-homing populations, respectively.

T_H17 skewing in the $CD4^+$ memory T cells of affected individuals

We next investigated the phenotype of $CD4^+$ memory T cells in affected individuals. Like other researchers,[23,24] we found that it was not possible to separate the different T helper cell subsets into specific subclusters. We therefore used SingleR to annotate T_H1, T_H2, and T_H17 cell identities within the existing $CD4^+$ T1 and $CD4^+$ T2 clusters. This revealed a significant enrichment of T_H17 lymphocytes among the memory $CD4^+$ T cells of PPP cases. The effect was observed in both the circulating ($CD4^+$ T1) and the skin-homing ($CD4^+$ T2) populations, but it was especially marked in the latter, where the median T_H17 fraction was 13.9% in cases versus 0.5% in controls ($P < 10^{-4}$) (Fig 3, *A,* and see Fig E4, *A,* in the Online Repository at www.jacionline.org). No further abnormalities were consistently observed in both memory $CD4^+$ compartments (Fig 3, *A,* and Fig E4, *A*).

To validate these findings with another methodology, we examined the T_H1, T_H2, and T_H17 transcriptional signatures developed by Cano-Gamez et al.[23] This confirmed that T_H17 gene expression was elevated in both circulating and skin-homing cells of affected individuals, while T_H1 and T_H2 scores were not (Fig E4, *B*). In keeping with these observations, an analysis of the transcription factors driving T_H1 (*TBX21*/T-bet), T_H2 (*GATA3*), and T_H17 (*RORG*/RORγt) lineage commitment demonstrated that *RORG* (but not *TBX21* or *GATA3*) was upregulated in the memory $CD4^+$ T cells of PPP patients (Fig 3, *B*). Of note, the overexpression of *RORG* was not replicated in memory $CD8^+$ T cells (Fig E4, *C*), which argues against a pathogenic involvement of Tc17 lymphocytes.

Taken together, these observations demonstrate a dominant T_H17 phenotype in the circulating memory $CD4^+$ T cells of people with PPP.

Increased T_H17 to T_H2 plasticity in the $CD4^+$ memory T cells of affected individuals

Given the different T-cell responses observed in PPP skin (T_H2 activation) and blood (T_H17 skewing), we investigated the possibility that T helper cell plasticity may contribute to disease pathogenesis. It is now well established that changes in the cytokine environment can modulate the identity of T_H17 cells and induce a shift toward T_H1 or T_H2 phenotypes.[25,26] We therefore sought to determine the extent of T_H17 cell plasticity in patients with PPP and in HCs.

We first queried the scRNA-Seq data generated in circulating and skin-homing $CD4^+$ memory T lymphocytes. Specifically, we searched for cells that expressed both *GATA3* and *KLRB1*/CD161, which we selected as readily detectable T_H2 and T_H17 markers. This identified a subset of $CD4^+$ memory T cells that expressed both genes. Unsupervised hierarchical clustering showed that the $GATA3^+/CD161^+$ cells were more closely related to T_H17 than T_H2 lymphocytes (Fig 4, *A*), as the expression of *RORG* and *IL23R* was readily detectable in dual-positive cells whereas the *IL4R* transcript levels were low (Fig 4, *B,* and see Fig E5, *A,* in the Online Repository at www.jacionline.org).

Although the simultaneous presence of GATA3 and CD161 has been documented in T_H2A cells (a T_H2 subtype associated with allergic disease[27]), our dual-positive population did not show well-established T_H2A markers such as *PPARG, PTGS2,* or *HPGDS*[27] (Fig 4, *B,* and Fig E5, *B*). T_H9 signature genes such as *SPI1*/PU.1 and *BATF*[28] were likewise weakly expressed (Fig 4, *B,* Fig E5, *B*). Conversely, the $GATA3^+/CD161^+$ cells in our data set had the same $CCR6^+/RORG^+/GATA3^+/CXCL8^+$ phenotype as a T_H17/T_H2 subset observed among patients with asthma.[29,30] Interestingly, Cosmi et al[29] showed that these T_H17/T_H2 cells can be derived from T_H17 ($CCR6^+/CD161^+$) lymphocytes in the presence of IL-4 and that they can acquire functional T_H2 characteristics (despite low *IL4R* expression) alongside their T_H17 phenotype.

Here, we further explored the correlation between $GATA3^+/CD161^+$ T_H17 and T_H2 cells by carrying out a pseudotime analysis of the entire $CD4^+$ T-cell compartment. Using Slingshot,[18] we found that $GATA3^+/CD161^+$ cells appeared later in pseudotime compared to both T_H17 and T_H2 cells (Fig 4, *C*). Of note, the expression of *GATA3* and *KLRB1*/CD161 continued to rise steadily during pseudotime, reflecting the pattern observed for T_H17 genes such as *RORC* and *IL23R*. Conversely, the levels of T_H2 markers such as *CXCR4* and *PTGDR2* peaked and then fell sharply (Fig 4, *D*). This is in keeping with the notion that the dual-positive cells differentiate from T_H17 rather than T_H2 lymphocytes.

We next investigated the pathogenic significance of the $CD161^+/GATA3^+$ population. We observed that the dual-positive cells were more abundant among the memory $CD4^+$ T cells of PPP cases compared to those of controls (13.7% vs 6.3%, $P = .004$) (Fig 4, *E*).

This difference was consistently observed among circulating ($CD4^+$ T1) and skin-homing ($CD4^+$ T2) T lymphocytes (Fig E5, *C*).

Thus, we have identified a T_H17/T_H2 population that is associated with PPP.

Experimental validation of increased T_H17 and T_H17/T_H2 cell abundance in PPP cases

We next sought to validate the scRNA-Seq findings by flow cytometry analysis of PBMCs obtained from 6 affected individuals and 6 healthy volunteers (including 4 cases and 4 controls that had not been included in the scRNA-Seq experiment). We found that the overall abundance of memory $CD4^+$ T cells and T_H17 cells was comparable in cases and controls (see Fig E6, *A* and *B,* in the Online Repository at www.jacionline.org). However, the frequency of T_H17 cells among skin-homing T lymphocytes was elevated in individuals with PPP (9.8% vs 5.2% in healthy volunteers; $P = .03$) (Fig 5, *A*), reflecting the pattern observed by scRNA-Seq. Likewise, T_H17/T_H2 cells were more abundant in affected compared to unaffected subjects. This effect was observed in the overall memory $CD4^+$ T cell compartment (9.1% vs 6.6%, $P = .009$) and also documented in the skin-homing population (6.1% vs 4.3% $P = .04$) (Fig 5, *B* and *C,* and Fig E6, *C*).

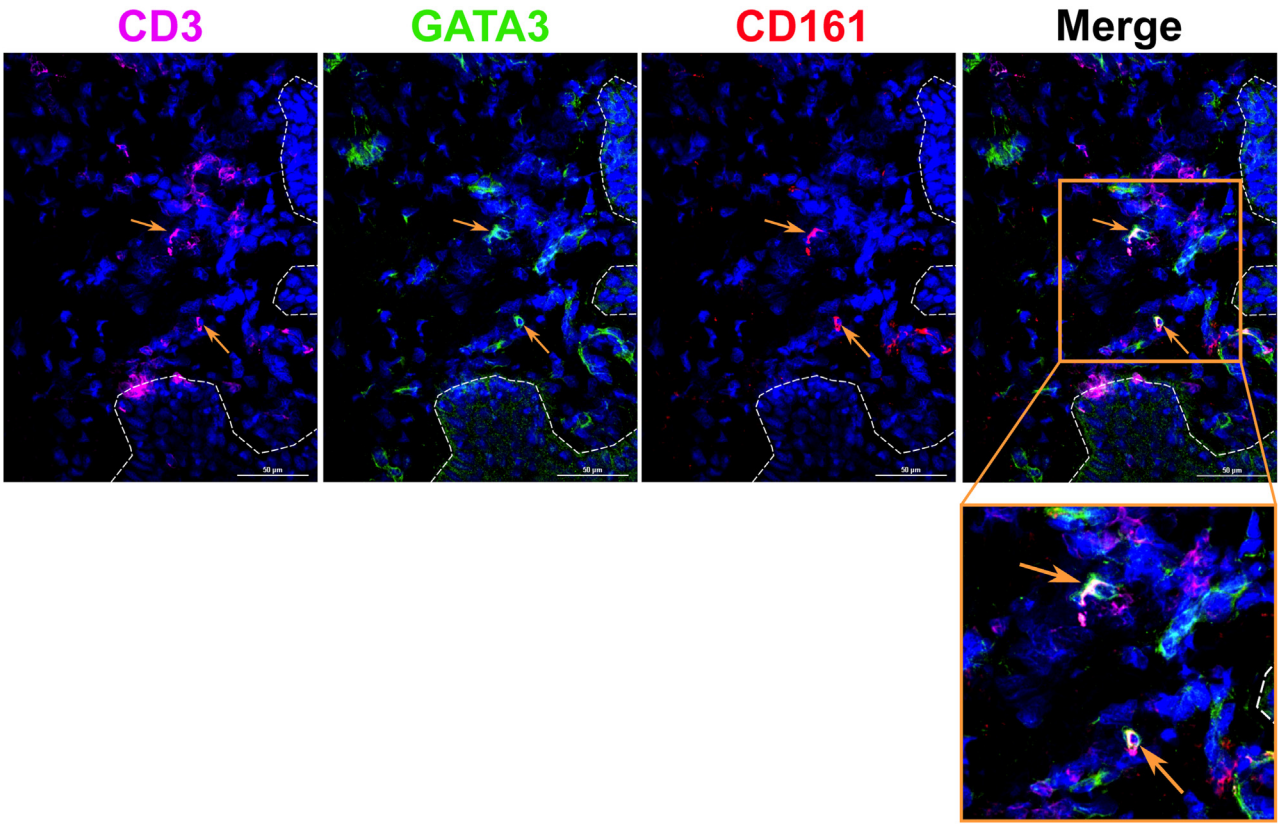

FIG 6. Immune fluorescence analysis of NL-PPP skin. A representative confocal microscopy image shows GATA3$^+$/CD161$^+$ T cells (*arrows*) infiltrating the upper dermis. Scale bars, 50 μm. The dermal–epidermal junction is indicated by a *dotted line*.

To further examine the pathogenic role of dual-positive cells, we carried out fluorescence microscopy in NL-PPP skin. We observed T-cell infiltration in the upper dermis, where GATA3$^+$/CD161$^+$ cells were clearly visible (Fig 6 and see Fig E7 in the Online Repository at www.jacionline.org).

Thus, dual-positive T_H17/T_H2 cells are overrepresented among the skin-homing CD4$^+$ T cells of affected individuals and readily detectable in their dermal infiltrates.

DISCUSSION

The purpose of this study was to achieve a better understanding of the immunologic determinants of PPP, a condition that remains poorly understood at the etiological level and recalcitrant to treatment in real-world practice.[1]

We applied hypothesis-free transcriptomic approaches to a tightly phenotyped PPP resource that met the rigorous inclusion criteria of the APRICOT clinical trial.[6] We focused on cells (circulating PBMCs) and tissues (NL skin) that were not affected by overt inflammation so that we could survey the immune landscape of the disease in an unbiased fashion. The advantages of this approach are exemplified by the results of the initial RNA-Seq experiment, where the comparison of lesional versus NL biopsy samples detected a predictable upregulation of innate pathways in involved skin. Conversely, the analysis of NL versus control samples revealed an unexpected and highly prominent signature of T-cell activation in uninvolved patient skin. The evidence for the activation of T_H2 lymphocytes was particularly significant, whereas the enrichment of T_H17-related pathways was relatively modest. This argues against the traditional classification of PPP as a clinical variant of plaque psoriasis[1] and highlights hitherto unsuspected similarities with atopic dermatitis.

The pathogenic involvement of T cells was also supported by the results obtained in circulating PBMCs. Because the use of Boolean flow cytometry gates cannot fully recapitulate the immune populations derived by scRNA-Seq cell clustering, there were some discrepancies between the results obtained with the 2 platforms. For example, scRNA-Seq experiments showed an increased frequency of the memory CD4$^+$ T1 and memory CD4$^+$ T2 clusters among affected individuals. Although the same trend was observed for the memory CD4$^+$ T cells detected by flow cytometry, the difference between cases and controls was not statistically significant.

Importantly, our key findings were validated in both platforms. Thus, scRNA-Seq and flow cytometry experiments consistently showed a skewed T_H17 phenotype for patient skin-homing T lymphocytes. They also demonstrated an increased abundance of T_H17/T_H2 (GATA3$^+$/CD161$^+$) cells among PPP cases.

To our knowledge, these results provide the first evidence of systemic abnormalities in PPP. They may also explain the common occurrence of extracutaneous, T-cell–mediated comorbidities (eg, psoriatic arthritis, autoimmune thyroid disease) among affected individuals.[3]

Our observation of increased T_H17/T_H2 cell abundance in PPP cases also suggests a pathogenic role for T_H17 plasticity. Interestingly, T_H17/T_H2 cells have been detected in the blood

and bronchoalveolar lavage of asthmatic individuals, where they have been characterized as IL-4/IL-17–producing cells.[29,30] A similar enrichment in patient populations has been reported for IL-17/IFN-γ–producing cells (T_H17/T_H1) in rheumatoid arthritis. Thus, T_H17 cells that are shifted toward T_H1 or T_H2 phenotypes are considered more pathogenic than their unshifted counterparts.[25,31] Intriguingly, T_H17 cell plasticity has also been associated with cigarette smoking,[32] one of the main risk factors for PPP.[2] Thus, several lines of evidence support the notion that the T_H17/T_H2 cells detected in the blood and skin of PPP patients contribute to disease processes.

It has been hypothesized that T_H17/T_H2 and T_H17/T_H1 cells originate in complex inflammatory milieus that cannot be easily recapitulated by *in vitro* polarization protocols.[25,26] This is in keeping with the multifaceted immune landscape we detected in PPP skin. Although the limitations of bulk RNA-Seq prevented us from characterizing these circuits, our analysis uncovered a clear upregulation of distinct cytokine networks.

The simultaneous activation of multiple immune pathways in PPP skin would also explain the limited therapeutic efficacy of biologic drugs that block single cytokines.[5] In fact, our results suggest that agents inhibiting diverse inflammatory pathways (eg, JAK inhibitors, which have been used with some success in individual PPP cases[33,34]) might deliver better clinical outcomes than targeted monoclonal antibodies. In this context, single-cell analysis of the signaling hubs that are deregulated in PPP (eg, the JAK1/JAK3 or JAK2/TYK2 complex) holds the promise of identifying novel therapeutic targets for this severe and disabling disease.

We are grateful to all the patients and volunteers who took part in this study.

In addition to A. David Burden, Christopher E. M. Griffiths, Nick J. Levell, Richard Parslew, Andrew E. Pink, Nick J. Reynolds, Richard B. Warren, Jonathan N. Barker, Catherine H. Smith, and Francesca Capon, who are authors, the following APRICOT and PLUM study team members facilitated patient recruitment and data processing for the APRICOT clinical trial and the PLUM study: David Baudry (Guy's Hospital, London), Victoria Cornelius (Imperial College London, London), Helen Lachmann (Royal Free Hospital, London), Helen McAteer (Psoriasis Association, Northampton), Freya Meynell (Guy's Hospital, London), Prakash Patel (Guy's Hospital, London), Angela Pushparajah (Guy's Hospital, London), and Rosemary Wilson (Guy's Hospital, London).

Clinical implications: The simultaneous activation of T_H17 and T_H2 responses in PPP supports the therapeutic use of agents that inhibit multiple T-cell pathways.

REFERENCES

1. Burden AD, Kirby B. Psoriasis and related disorders. In: Griffiths CEM, Barker JN, Bleiker T, Chalmers RJ, Creamer D, editors. Rook's textbook of dermatology. Chichester (UK): Wiley-Blackwell; 2016.
2. Twelves S, Mostafa A, Dand N, Burri E, Farkas K, Wilson R, et al. Clinical and genetic differences between pustular psoriasis subtypes. J Allergy Clin Immunol 2019;143:1021-6.
3. Benzian-Olsson N, Dand N, Chaloner C, Bata-Csorgo Z, Borroni R, Burden AD, et al. Association of clinical and demographic factors with the severity of palmoplantar pustulosis. JAMA Dermatol 2020;156:1216-22.
4. Mossner R, Frambach Y, Wilsmann-Theis D, Lohr S, Jacobi A, Weyergraf A, et al. Palmoplantar pustular psoriasis is associated with missense variants in CARD14, but not with loss-of-function mutations in IL36RN in European patients. J Invest Dermatol 2015;135:2538-41.
5. Obeid G, Do G, Kirby L, Hughes C, Sbidian E, Le Cleach L. Interventions for chronic palmoplantar pustulosis: abridged Cochrane systematic review and GRADE assessments. Br J Dermatol 2021;184:1023-32.
6. Cro S, Cornelius VR, Pink AE, Wilson R, Pushpa-Rajah A, Patel P, et al. Anakinra for palmoplantar pustulosis: results from a randomized, double-blind, multicentre, two staged, adaptive placebo controlled trial (APRICOT). Br J Dermatol 2021;186:245-56.
7. Mrowietz U, Burden AD, Pinter A, Reich K, Schakel K, Baum P, et al. Spesolimab, an anti-interleukin-36 receptor antibody, in patients with palmoplantar pustulosis: results of a phase IIa, multicenter, double-blind, randomized, placebo-controlled pilot study. Dermatol Ther (Heidelb) 2021;11:571-85.
8. Mrowietz U, Bachelez H, Burden AD, Rissler M, Sieder C, Orsenigo R, et al. Secukinumab for moderate-to-severe palmoplantar pustular psoriasis: results of the 2PRECISE study. J Am Acad Dermatol 2019;80:1344-52.
9. Terui T, Kobayashi S, Okubo Y, Murakami M, Zheng R, Morishima H, et al. Efficacy and safety of guselkumab in Japanese patients with palmoplantar pustulosis: a phase 3 randomized clinical trial. JAMA Dermatol 2019;155:1153-61.
10. Navarini AA, Burden AD, Capon F, Mrowietz U, Puig L, Koks S, et al. European consensus statement on phenotypes of pustular psoriasis. J Eur Acad Dermatol Venereol 2017;31:1792-9.
11. Wohnhaas CT, Leparc GG, Fernandez-Albert F, Kind D, Gantner F, Viollet C, et al. DMSO cryopreservation is the method of choice to preserve cells for droplet-based single-cell RNA sequencing. Sci Rep 2019;9:10699.
12. Zheng GX, Terry JM, Belgrader P, Ryvkin P, Bent ZW, Wilson R, et al. Massively parallel digital transcriptional profiling of single cells. Nat Commun 2017;8:14049.
13. Schafflick D, Xu CA, Hartlehnert M, Cole M, Schulte-Mecklenbeck A, Lautwein T, et al. Integrated single cell analysis of blood and cerebrospinal fluid leukocytes in multiple sclerosis. Nat Commun 2020;11:247.
14. Korsunsky I, Millard N, Fan J, Slowikowski K, Zhang F, Wei K, et al. Fast, sensitive and accurate integration of single-cell data with Harmony. Nat Methods 2019;16:1289-96.
15. Stuart T, Butler A, Hoffman P, Hafemeister C, Papalexi E, Mauck WM 3rd, et al. Comprehensive integration of single-cell data. Cell 2019;177:1888-902.e21.
16. Aran D, Looney AP, Liu L, Wu E, Fong V, Hsu A, et al. Reference-based analysis of lung single-cell sequencing reveals a transitional profibrotic macrophage. Nat Immunol 2019;20:163-72.
17. Monaco G, Lee B, Xu W, Mustafah S, Hwang YY, Carre C, et al. RNA-Seq signatures normalized by mRNA Abundance allow absolute deconvolution of human immune cell types. Cell Rep 2019;26:1627-16240.e7.
18. Street K, Risso D, Fletcher RB, Das D, Ngai J, Yosef N, et al. Slingshot: cell lineage and pseudotime inference for single-cell transcriptomics. BMC Genomics 2018;19:477.
19. Tsoi LC, Rodriguez E, Degenhardt F, Baurecht H, Wehkamp U, Volks N, et al. Atopic dermatitis is an IL-13–dominant disease with greater molecular heterogeneity compared to psoriasis. J Invest Dermatol 2019;139:1480-9.
20. Garcia G, Godot V, Humbert M. New chemokine targets for asthma therapy. Curr Allergy Asthma Rep 2005;5:155-60.
21. Homey B, Steinhoff M, Ruzicka T, Leung DY. Cytokines and chemokines orchestrate atopic skin inflammation. J Allergy Clin Immunol 2006;118:178-89.
22. Klicznik MM, Morawski PA, Hollbacher B, Varkhande SR, Motley SJ, Kuri-Cervantes L, et al. Human $CD4^+CD103^+$ cutaneous resident memory T cells are found in the circulation of healthy individuals. Sci Immunol 2019;4:eaav8995.
23. Cano-Gamez E, Soskic B, Roumeliotis TI, So E, Smyth DJ, Baldrighi M, et al. Single-cell transcriptomics identifies an effectorness gradient shaping the response of $CD4^+$ T cells to cytokines. Nat Commun 2020;11:1801.
24. Kiner E, Willie E, Vijaykumar B, Chowdhary K, Schmutz H, Chandler J, et al. Gut $CD4^+$ T cell phenotypes are a continuum molded by microbes, not by TH archetypes. Nat Immunol 2021;22:216-28.
25. Stockinger B, Omenetti S. The dichotomous nature of T helper 17 cells. Nat Rev Immunol 2017;17:535-44.
26. Tortola L, Jacobs A, Pohlmeier L, Obermair FJ, Ampenberger F, Bodenmiller B, et al. High-dimensional T helper cell profiling reveals a broad diversity of stably committed effector states and uncovers interlineage relationships. Immunity 2020;53:597-613.e6.
27. Wambre E, Bajzik V, DeLong JH, O'Brien K, Nguyen QA, Speake C, et al. A phenotypically and functionally distinct human T_H2 cell subpopulation is associated with allergic disorders. Sci Transl Med 2017;9:eaam9171.
28. Jabeen R, Goswami R, Awe O, Kulkarni A, Nguyen ET, Attenasio A, et al. Th9 cell development requires a BATF-regulated transcriptional network. J Clin Invest 2013;123:4641-53.
29. Cosmi L, Maggi L, Santarlasci V, Capone M, Cardilicchia E, Frosali F, et al. Identification of a novel subset of human circulating memory $CD4^+$ T cells that produce both IL-17A and IL-4. J Allergy Clin Immunol 2010;125:222-30.e1-4.
30. Irvin C, Zafar I, Good J, Rollins D, Christianson C, Gorska MM, et al. Increased frequency of dual-positive T_H2/T_H17 cells in bronchoalveolar lavage fluid characterizes a population of patients with severe asthma. J Allergy Clin Immunol 2014;134:1175-86.e7.

31. Cosmi L, Santarlasci V, Maggi L, Liotta F, Annunziato F. Th17 plasticity: pathophysiology and treatment of chronic inflammatory disorders. Curr Opin Pharmacol 2014;17:12-6.
32. Xu W, Li R, Sun Y. Increased IFN-gamma–producing Th17/Th1 cells and their association with lung function and current smoking status in patients with chronic obstructive pulmonary disease. BMC Pulm Med 2019;19:137.
33. Koga T, Sato T, Umeda M, Fukui S, Horai Y, Kawashiri SY, et al. Successful treatment of palmoplantar pustulosis with rheumatoid arthritis, with tofacitinib: impact of this JAK inhibitor on T-cell differentiation. Clin Immunol 2016;173:147-8.
34. Mossner R, Hoff P, Mohr J, Wilsmann-Theis D. Successful therapy of palmoplantar pustulosis with tofacitinib—report on three cases. Dermatol Ther 2020;33:e13753.